

Toolbox for continuous-variable entanglement production and measurement using spontaneous parametric down-conversion

G. Boucher,^{1,*} T. Douce,¹ D. Bresteau,^{1,†} S. P. Walborn,² A. Keller,³ T. Coudreau,¹ S. Ducci,¹ and P. Milman¹

¹Laboratoire Matériaux et Phénomènes Quantiques, Université Paris Diderot, CNRS UMR 7162, 75013, Paris, France

²Instituto de Física, Universidade Federal do Rio de Janeiro, Caixa Postal 68528, 21941-972 Rio de Janeiro, RJ, Brazil

³Institut de Sciences Moléculaires d'Orsay (CNRS), Université Paris-Sud 11, Bâtiment 350–Campus d'Orsay, 91405 Orsay Cedex, France

(Received 9 April 2015; published 4 August 2015)

We provide a toolbox for continuous-variable quantum-state engineering and characterization of biphoton states produced by spontaneous parametric down-conversion in a transverse pump configuration. We show that the control of the pump beam's incidence spot and angle corresponds to phase-space displacements of conjugate collective continuous variables of the biphoton. In particular, we illustrate with numerical simulations on a semiconductor device how this technique can be used to engineer and characterize arbitrary states of the frequency and time degrees of freedom.

DOI: [10.1103/PhysRevA.92.023804](https://doi.org/10.1103/PhysRevA.92.023804)

PACS number(s): 42.50.Dv, 03.67.Bg, 42.65.Lm, 42.65.Wi

I. INTRODUCTION

Spontaneous parametric down-conversion (SPDC) experiments play a prominent role in the field of quantum information and communications. Single and multiple photon pairs generated through SPDC display entanglement in multiple degrees of freedom (DOF) which are fundamentally different from each other. When combined or independently accessed, they constitute a powerful platform for experimental demonstrations of quantum protocols. Discrete DOF, such as polarization and orbital angular momentum, are currently used to implement quantum logic gates and protocols [1], test the nonlocal properties of quantum mechanics [2–5], and realize quantum cryptography [6–8] and teleportation [9,10]. DOF associated with observables with a continuous spectrum, like the quadratures of the electromagnetic field, potentially offer the same versatility as discrete ones in the field of quantum information. Continuous DOF in the single-photon regime, such as frequency, transverse momentum, or position, display a perfect analogy with a multiphoton single-mode continuous variable (CV) [11,12]. Consequently, they constitute an attractive platform to realize CV quantum information protocols [13] that are usually associated with the single-mode multiphoton configuration. For example, an appealing aspect of using a single photon's transverse coordinates in this field is their relatively easy manipulation with readily available optical devices, such as spatial light modulators (SLMs) and lenses [12], circumventing the difficulties encountered in multiphoton CV strategies to implement non-Gaussian operations, which are essential ingredients of universal quantum computation [13]. For these reasons, the study of entanglement in CVs in the single-photon regime is a valuable strategy to demonstrate CV-based quantum gates [14], quantum key distribution [15,16], error correcting codes [17,18], and quantum metrology protocols [19] and to study quantum-to-classical transitions [20,21]. Finally, we can

mention that continuous DOF can be combined with discrete ones to implement conditional operations [22–24].

CV entanglement in photon pairs can be generated in different DOF via SPDC; one example is the spatial transverse DOF of photon pairs produced in nonlinear bulk crystals. Tailoring the spatial properties of the pump beam has been previously employed to engineer [25,26] and detect quantum states of photon pairs with different properties: in [27] it was shown that controlling the transverse phase properties of the pump beam could lead to bunching or antibunching of a photon pair. References [22] and [28] demonstrate that the use of SLMs placed in the arms of an interferometer can lead to the measurement of arbitrary momenta of the quantum state associated with the transverse photonic DOF.

Using frequency as a CV degree of freedom instead of the transverse coordinates presents a series of potential advantages: in general, the transverse variables of a propagating field are entangled in the two-dimensional orthogonal spatial coordinates x and y or, equivalently, the momentum coordinates p_x and p_y ; this renders arbitrary state production and measurement more challenging and limits the applications of such DOF in quantum information tasks, since the quantum state associated with each spatial direction is entangled and can be cross-correlated between the x and the y directions. Moreover, this spatial entanglement is jeopardized when coupling into optical fibers or waveguides, while frequency states remain robust in such devices. For all these reasons, we illustrate our ideas focusing on the spectral degree of freedom. Indeed, the characterization of arbitrary frequency entangled states of photon pairs draws a lot of attention as illustrated by recent works on frequency-dependent intensity correlation measurements of the photon pair [29], the reconstruction of biphoton wave functions generated with a monochromatic pump [30], and amplitude-sensitive tomography techniques in the time-energy space [31].

In the waveguided regime, frequency-correlated, uncorrelated, and anticorrelated photon pairs can be produced by modifying the spectral properties of the pump beam [32,33]. Nevertheless, even if the nature of correlations can be controlled, pump bandwidth modification alone cannot lead to arbitrary CV-state engineering, an essential tool for CV

*guillaume.boucher@univ-paris-diderot.fr

†Current address: Laboratoire Aimé Cotton, Bâtiment 505–Campus d'Orsay, Université Paris-Sud 11, 91405 Orsay Cedex, France.

quantum information and communications, fundamental tests of quantum mechanics and quantum metrology.

In this paper, we provide a toolbox to exploit the capabilities of SPDC to create, measure, and characterize entanglement in the CV DOF of a photon pair. Our strategy is based on the combination of pump spatial engineering with the possibility of characterizing a Wigner function of the photon pair using a Hong-Ou-Mandel (HOM)-type [34] experiment [35].

In order to clarify these concepts, we present the case study of a transversally pumped semiconductor waveguide [36,37] potentially having great versatility in the control of the biphoton frequency correlations [29]. Indeed it has been shown that the pumping configuration allows one to modify the phase matching conditions by simply changing the spatial properties of the pump beam [38–40], e.g., its waist or angle of incidence. However, more complex quantum-state engineering has not been explored so far.

II. DESCRIPTION OF THE BIPHOTON STATE WITH CHRONOCYCLIC WIGNER FUNCTIONS

The properties of the photon pair are described by the biphoton wave function, which takes a complex form due to the constraints imposed by momentum and energy conservation. By neglecting group velocity dispersion (which is justified in the spectral range of the generated photon pairs) and in the narrow-bandwidth limit for the pump beam, we can write the state of the pair in the form

$$|\Psi\rangle = \chi_\Gamma \iint d\omega_s d\omega_i f_+(\omega_s + \omega_i) f_-(\omega_s - \omega_i) |\omega_s, \omega_i\rangle, \quad (1)$$

where $\omega_{s,i}$ represent the signal and idler frequencies, respectively, and χ_Γ is a normalization constant [41]. The function f_+ corresponds to the spectrum of the pump beam reflecting the condition of energy conservation ($\omega_p = \omega_s + \omega_i \equiv \omega_+$). The phase of this function is affected by the presence of a microcavity formed by two Bragg mirrors as shown in the nonflat phase profile in Fig. 1(c). The narrow-band assumption allows us to consider the phase-matching-dependent part of the biphoton state as a strictly antidiagonal function f_- ,

$$f_-(\omega_- \equiv \omega_s - \omega_i) = \int_{-L/2}^{L/2} dz \varphi(z) e^{i \frac{(\omega_s - \omega_i)z}{\bar{v}_g}}, \quad (2)$$

where L is the length of the sample, \bar{v}_g is the average group velocity of the signal and idler photons at frequency degeneracy, and $\varphi(z) = \Phi(z) e^{-ik_{\text{deg}} z}$. The function $\Phi(z)$ is the spatial profile of the pump beam and $k_{\text{deg}} = \sin(\theta_{\text{deg}}) \frac{\omega_p^{(0)}}{c} = \frac{(n_s - n_i)}{2} \frac{\omega_p^{(0)}}{c}$, where $n_{s,i}$ corresponds to the signal and idler effective refractive indices at degeneracy, $\omega_p^{(0)}$ is the central frequency of the pump beam, and θ_{deg} is the pumping incidence angle for which degeneracy occurs.

If the dimensions of the waveguide are large with respect to the pump waist, i.e., the limit where $L \rightarrow \infty$, f_- can be approximated by the Fourier transform of the spatial profile of the pump beam:

$$f_-(\omega_-) \approx \tilde{\varphi}\left(\frac{\omega_-}{\bar{v}_g}\right). \quad (3)$$

We start by considering the situation depicted in Fig. 1(a), where a Gaussian pump beam with waist w_p impinges onto the source at an angle θ and position z_0 . The field distribution along the axis z is $\Phi(z) \propto e^{-(z-z_0)^2 \cos^2 \theta / w_p^2} e^{i(k \sin \theta)z}$ and therefore f_- reads

$$f_-(\omega_-) \propto e^{i\omega_- \tau_0} e^{-\frac{(\omega_- - \omega_-^{(0)})^2}{\Delta\omega^2}}, \quad (4)$$

with $\tau_0 = z_0/\bar{v}_g$, $\Delta\omega = \bar{v}_g/2w_p$, and $\omega_-^{(0)} = (k \sin \theta - k_{\text{deg}})\bar{v}_g \approx \delta\theta \bar{v}_g \omega_p/c$ [42]. Figures 1(b) and 1(c) represent the biphoton wave-function norm and phase distribution numerically simulated for a pump impinging at the degeneracy angle θ_{deg} at $z_0 = 0$ with waist $w_p = 200 \mu\text{m} \ll L = 2 \text{ mm}$, central wavelength $\lambda_p = 775 \text{ nm}$, and pulse duration $\tau_p = 3.2 \text{ ps}$ [43].

Instead of the complex-valued biphoton wave function, a more convenient representation is given by chronocyclic Wigner functions, which are the time-energy analogs of the phase-space Wigner functions. With this approach, the time and energy properties of the single photons of the pairs are illustrated with real quantities [44,45], in the same way that pulses of light are depicted in the domain of ultrafast optics [46]. In this work, we describe, instead of the properties of the isolated photons of the pair, their correlations along the antidiagonal part f_- of the biphoton wave function. This represents the quasiprobability distribution of the biphoton as a function of the detuning Ω between signal and idler frequencies and the time-delay-conjugated variable τ . The corresponding Wigner function W_- is given by

$$W_-(\tau, \Omega) = \int_{-\infty}^{\infty} d\omega_- f_-(\Omega - \omega_-) f_-^*(\Omega + \omega_-) e^{i2\tau\omega_-}. \quad (5)$$

Using the expression obtained in (4), we see that this corresponds to a Gaussian Wigner function centered at point $\tau = \tau_0$, $\Omega = \omega_-^{(0)}$, of widths $\Delta\Omega = 1/\Delta\tau = \Delta\omega = \bar{v}_g/2w_p$, which is equivalent to the representation of a coherent state [see Fig. 1(d)]. Thus, in this situation, shifting the pumping spot z_0 is equivalent to realizing displacements in the τ axis of the phase space, while changing the angle of incidence θ of the pump beam corresponds to shifting the state along the Ω axis.

III. ENGINEERING AND MEASUREMENT OF BIPHOTON STATES

More complex states can be obtained by engineering the pump beam. Indeed two identical beams impinging at z_a and z_b will generate a superposition of two coherent states displaced along the τ axis. In the limit $|z_a - z_b| \gg 2w_p$ such states are almost orthogonal, representing a superposition of two distinct quasiclassical states (Schrödinger cat-like states). An analog superposition is obtained along axis Ω by using two angles of incidence, θ_a and θ_b , impinging at the same point z_0 . Quasiorthogonality is obtained for $|\theta_a - \theta_b| \gg \frac{c}{2\omega_p w_p}$. We can generalize these Schrödinger cat-like states using more complex configurations of pump beams. As an illustration, we choose a compass state (see Fig. 2), a superposition of four coherent states presenting interesting applications in quantum metrology, as pointed out in [47] and [48]. In order to obtain this state, a set of four different pump beam configurations is required: two pairs of beams impinging at two different points

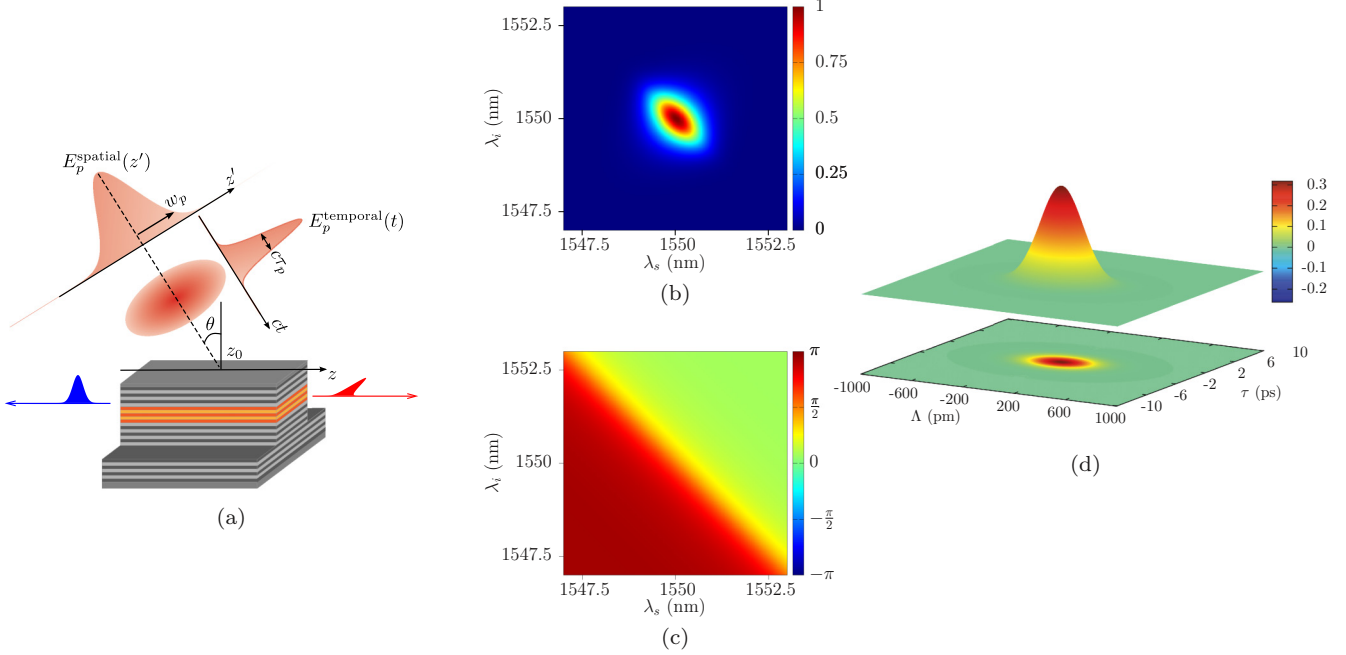


FIG. 1. (Color online) (a) Counter-propagating phase-matching scheme implemented in a semiconductor microcavity waveguide. The characteristics of the pump pulses allow us to tune the time-energy properties of the biphoton. (b) Norm and (c) phase of the biphoton wave function for $w_p = 200 \mu\text{m}$, $\lambda_p = 775 \text{ nm}$, $\tau_p = 3.2 \text{ ps}$, and $\theta = \theta_{\text{deg}}$. The phase pattern in (c) is due to the resonance of the pump in the microcavity. (d) Corresponding Wigner function. The Ω axis is given in units of $\Omega = \frac{8\pi c}{\omega_p^2} \Omega$.

separated by a distance Δz , each pair consisting of two beams tilted symmetrically with respect to the degeneracy angle as shown in Fig. 2(a).

The procedure detailed above to generate quantum states with different properties and applications can be generalized, leading to the creation of arbitrary CV quantum states, since

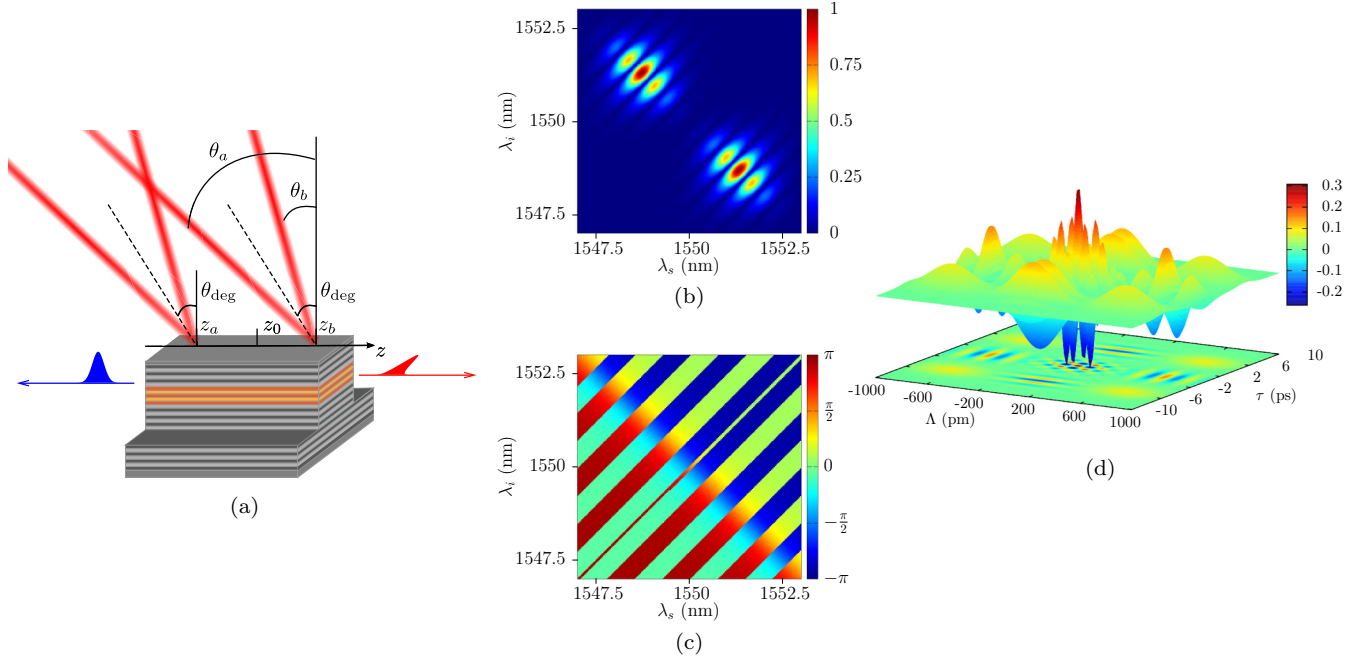


FIG. 2. (Color online) (a) Pump illumination scheme to generate a compass state: two pairs of beams impinge onto the waveguide at two spots, z_a and z_b , equidistant from the center of the source, each pair consisting of two beams tilted symmetrically with respect to the degeneracy angle ($\theta_{a,b} = \theta_{\text{deg}} \pm \delta\theta$). (b) Norm and (c) phase of the biphoton wave function of the corresponding cat state with $\delta\theta = 9.37'$, $|z_a - z_b| = 1 \text{ mm}$ and for each beam $w_p = 200 \mu\text{m}$, $\lambda_p = 775 \text{ nm}$, $\tau_p = 3.2 \text{ ps}$, and $\theta = \theta_{\text{deg}}$. (d) Corresponding Wigner function with $\Delta\Lambda = 1.37 \text{ nm}$ and $\Delta\tau = 10.8 \text{ ps}$. The Ω axis is given in units of $\Omega = \frac{8\pi c}{\omega_p^2} \Omega$.

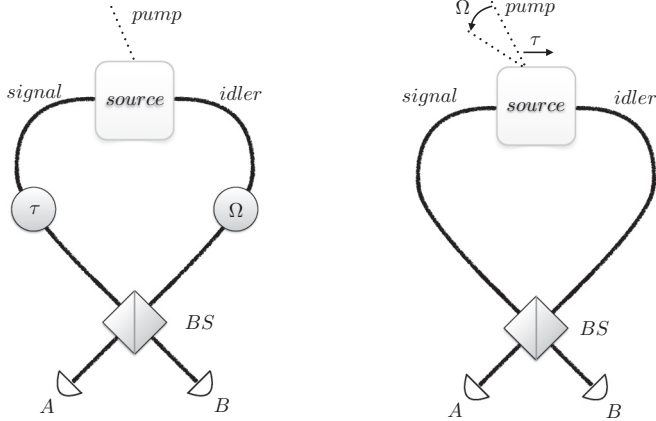


FIG. 3. Two possible strategies to realize the modified HOM experiment leading to the measurement of the Wigner function. Left: Displacements in time and frequency are realized in each arm of the interferometer after the production of the photon pair. Right: In a completely analogous setup, displacements in time and frequency are realized by pump engineering. While modifying the incidence angle of the pump beam, and, consequently, the phase matching condition, corresponds to displacements in frequency, modifying the pump's incidence spot corresponds to displacements in time.

any state can be constructed from the overcomplete basis of coherent states.

We now discuss how pump engineering can be used to characterize arbitrary CV states using the direct measurement of the Wigner function in all points of phase space. In [35], it was shown how a generalization of the HOM experiment leads to direct measurement of the Wigner function in the Ω, τ phase space. This generalization consists of considering displacements in the frequency degree of freedom of the photons, in addition to time displacements. Of course, displacing either one of these parameters modifies the distinguishability between the photons in each arm of the HOM interferometer, as depicted in Fig. 3. Time displacements can be realized relatively straightforwardly by simply modifying the optical path in each arm of the HOM interferometer. However, the frequency displacements required to reconstruct the Wigner function are quite broad with respect to the performances of currently available optical modulators [49]. Pump engineering provides an alternative solution to realize both time and frequency displacements, dramatically simplifying the direct measurement of the Wigner function and the CV state characterization.

As discussed previously, modification of the pump beam's incidence angle corresponds to displacing the central frequency of the symmetric part of the wave function associated with the photon pairs, while modification of the incidence point corresponds to time displacements. Using these ingredients, one can devise a procedure for the complete Wigner function measurement as follows: in the first step, an initial state is engineered. This state is the one to be characterized. Running the HOM experiment with no frequency or time displacement leads directly to the value of $W_{-}(0,0)$, the Wigner function at the origin [35]. Then tilting the incident pump beams by

a given amount and repeating the same HOM experiment is equivalent to displacing the original state in frequency and measuring its Wigner function, leading to the value of $W_{-}(\Omega,0)$. Analogously, displacing the pump beam in the z axis and repeating the HOM strategy leads to the value of $W_{-}(0,\tau)$. It is clear that, by combining different tilting angles and displacements, one can obtain an arbitrary point of the Wigner function and reconstruct $W_{-}(\Omega,\tau)$ for all values of Ω and τ . In order to characterize the quantum state, the magnitude of the displacements in both axes of phase space should cover the region where $|f_{-}(\omega_{-})|^2$ has a significant value. This corresponds to realizing the pump's angular displacements in an interval $\Delta\theta \approx \theta_a - \theta_b = 18.7'$, while its impinging position is displaced by an amount $\Delta z \approx z_a - z_b = 1$ mm (see Fig. 2). Note that, as shown in [50], the proposed strategy presents the advantage of not being limited by the detector's response time for measuring highly oscillating fringes or phase-space structures associated with sub-Planck scales [47]. Note that the resolution required for displacements along the z axis is easily achieved; as far as the angular displacement is concerned, since $\Delta\theta$ is of the order of 2.7 mrad, a resolution of 100 μ rad is sufficient to resolve the fringes. This is also achievable with thermal stabilization and stable mechanical mountings.

One may argue that modifying the pump, in reality, modifies the state to be measured instead of the measuring apparatus that is probing different points of the phase space; but this is common practice in quantum measurement strategies, where the modification of the settings of the measurement apparatus is formally equivalent to that of the state to be measured. This equivalency was used, for instance, in the context of cavity quantum electrodynamics in [21]. There, the Wigner function is directly measured using a Rydberg atom interacting dispersively for a fixed time interval with the field of a high-quality microwave cavity. The setup is kept the same for all points in phase space and the quantum state of the field in the cavity to be measured is displaced, and consequently modified, through the application of a coherent field. Also in [30], the use of a monochromatic pump generating pairs of photons through SPDC is combined with modification of the pump frequency (or shifts in the temperature of the crystal) to circumvent the difficulty of broad frequency displacements. In the present case, changing the pump spatial configuration is equivalent to displacing the state to be measured.

IV. CONCLUSION

In conclusion, we have shown how spatial pump engineering can be used to generate arbitrary CV frequency states of a photon pair and directly characterize it through a HOM-like experiment. The combination of the variety of pumping geometries with that of the possible design of integrated photonic circuits [51] will allow the realization of complex and versatile quantum photonic chips [40]. The generalization of this technique to prepare quantum states with higher photon numbers, as well as to simulate the dynamics of CV states and the application of different quantum operations to it, is an interesting open perspective that will be investigated.

ACKNOWLEDGEMENTS

This work was partly supported by the ANR project Semi-QuantRoom ANR-14-CE26-0029 and by Region Ile de France

in the framework of C'Nano IdF with the GENESIS project. S.D. acknowledges the Institut Universitaire de France. G.B. and T.D. contributed equally to this work.

- [1] J. L. O'Brien, *Science* **318**, 1567 (2007).
- [2] J. S. Bell, *Physics* **1**, 195 (1964).
- [3] J. F. Clauser, M. A. Horne, A. Shimony, and R. A. Holt, *Phys. Rev. Lett.* **23**, 880 (1969).
- [4] A. Aspect, P. Grangier, and G. Roger, *Phys. Rev. Lett.* **49**, 91 (1982).
- [5] R. Ursin, F. Tiefenbacher, T. Schmitt-Manderbach, H. Weier, T. Scheidl, M. Lindenthal, B. Blauensteiner, T. Jennewein, J. Perdigues, P. Trojek, B. Omer, M. Furst, M. Meyenburg, J. Rarity, Z. Sodnik, C. Barbieri, H. Weinfurter, and A. Zeilinger, *Nature Phys.* **3**, 481 (2007).
- [6] T. Jennewein, C. Simon, G. Weihs, H. Weinfurter, and A. Zeilinger, *Phys. Rev. Lett.* **84**, 4729 (2000).
- [7] D. S. Naik, C. G. Peterson, A. G. White, A. J. Berglund, and P. G. Kwiat, *Phys. Rev. Lett.* **84**, 4733 (2000).
- [8] N. Gisin, G. Ribordy, W. Tittel, and H. Zbinden, *Rev. Mod. Phys.* **74**, 145 (2002).
- [9] C. H. Bennett, G. Brassard, C. Crépeau, R. Jozsa, A. Peres, and W. K. Wootters, *Phys. Rev. Lett.* **70**, 1895 (1993).
- [10] D. Bouwmeester, J.-W. Pan, K. Mattle, M. Eibl, H. Weinfurter, and A. Zeilinger, *Nature (London)* **390**, 575 (1997).
- [11] A. F. Abouraddy, T. Yarnall, B. E. A. Saleh, and M. C. Teich, *Phys. Rev. A* **75**, 052114 (2007).
- [12] D. S. Tasca, R. M. Gomes, F. Toscano, P. H. Souto Ribeiro, and S. P. Walborn, *Phys. Rev. A* **83**, 052325 (2011).
- [13] S. L. Braunstein and P. van Loock, *Rev. Mod. Phys.* **77**, 513 (2005).
- [14] S. Lloyd and S. L. Braunstein, *Phys. Rev. Lett.* **82**, 1784 (1999).
- [15] F. Grosshans and P. Grangier, *Phys. Rev. Lett.* **88**, 057902 (2002).
- [16] F. Grosshans, G. Van Assche, J. Wenger, R. Brouri, N. J. Cerf, and P. Grangier, *Nature* **421**, 238 (2003).
- [17] D. Gottesman, A. Kitaev, and J. Preskill, *Phys. Rev. A* **64**, 012310 (2001).
- [18] O. J. Farías, F. de Melo, P. Milman, and S. P. Walborn, *Phys. Rev. A* **91**, 062328 (2015).
- [19] V. Giovannetti, S. Lloyd, and L. Maccone, *Phys. Rev. Lett.* **96**, 010401 (2006).
- [20] W. Zurek, *Phys. Today* **44**, 36 (1991).
- [21] S. Deléglise, I. Dotsenko, C. Sayrin, J. Bernu, M. Brune, J.-M. Raimond, and S. Haroche, *Nature (London)* **455**, 510 (2008).
- [22] M. Hor-Meyll, J. O. de Almeida, G. B. Lemos, P. H. S. Ribeiro, and S. P. Walborn, *Phys. Rev. Lett.* **112**, 053602 (2014).
- [23] P. Vernaz-Gris, A. Ketterer, A. Keller, S. P. Walborn, T. Coudreau, and P. Milman, *Phys. Rev. A* **89**, 052311 (2014).
- [24] J. Anders, D. K. L. Oi, E. Kashefi, D. E. Browne, and E. Andersson, *Phys. Rev. A* **82**, 020301 (2010).
- [25] C. H. Monken, P. H. S. Ribeiro, and S. Pádua, *Phys. Rev. A* **57**, 3123 (1998).
- [26] A. Valencia, A. Ceré, X. Shi, G. Molina-Terriza, and J. P. Torres, *Phys. Rev. Lett.* **99**, 243601 (2007).
- [27] S. P. Walborn, A. N. de Oliveira, S. Pádua, and C. H. Monken, *Phys. Rev. Lett.* **90**, 143601 (2003).
- [28] S. Machado, P. Milman, and S. P. Walborn, *Phys. Rev. A* **87**, 053834 (2013).
- [29] A. Eckstein, G. Boucher, A. Lemaître, P. Filloux, I. Favero, G. Leo, J. E. Sipe, M. Liscidini, and S. Ducci, *Laser Photon. Rev.* **8**, L76 (2014).
- [30] N. Tischler, A. Buese, L. G. Helt, M. L. Juan, N. Piro, J. Ghosh, M. J. Steel, and G. Molina-Terriza, [arXiv:1503.08629](https://arxiv.org/abs/1503.08629).
- [31] M. Avenhaus, B. Brecht, K. Laiho, and C. Silberhorn, [arXiv:1406.4252](https://arxiv.org/abs/1406.4252).
- [32] A. Eckstein, A. Christ, P. J. Mosley, and C. Silberhorn, *Phys. Rev. Lett.* **106**, 013603 (2011).
- [33] Y.-W. Cho, K.-K. Park, J.-C. Lee, and Y.-H. Kim, *Phys. Rev. Lett.* **113**, 063602 (2014).
- [34] C. K. Hong, Z. Y. Ou, and L. Mandel, *Phys. Rev. Lett.* **59**, 2044 (1987).
- [35] T. Douce, A. Eckstein, S. P. Walborn, A. Z. Khoury, S. Ducci, A. Keller, T. Coudreau, and P. Milman, *Sci. Rep.* **3**, 3530 (2013).
- [36] A. Orieux, X. Caillet, A. Lemaître, P. Filloux, I. Favero, G. Leo, and S. Ducci, *J. Opt. Soc. Am. B* **28**, 45 (2011).
- [37] A. Orieux, A. Eckstein, A. Lemaître, P. Filloux, I. Favero, G. Leo, T. Coudreau, A. Keller, P. Milman, and S. Ducci, *Phys. Rev. Lett.* **110**, 160502 (2013).
- [38] X. Caillet, V. Berger, G. Leo, and S. Ducci, *J. Mod. Opt.* **56**, 232 (2009).
- [39] J. Peřina, *Phys. Rev. A* **77**, 013803 (2008).
- [40] Z. D. Walton, A. V. Sergienko, B. E. A. Saleh, and M. C. Teich, *Phys. Rev. A* **70**, 052317 (2004).
- [41] The overlap between the field in the transverse and that in the epitaxial direction of the waveguide is contained in this term. The variations of χ_Γ with the pump, signal, and idler frequencies are negligible in the range of this study.
- [42] The transverse size of the pump beam will change with the incidence angle. However, the range of angles considered here is small enough to approximate $\sin \theta \rightarrow \theta$ and $\cos \theta \rightarrow 1$.
- [43] This choice of parameters corresponds to typical experimental conditions for the device illustrating our method. In particular, the generation of frequency-uncorrelated biphoton states is achievable by modifying the size pump beam so that f_+ and f_- have similar widths. Note that the technique remains valid for other pumping regimes since the pulse duration only impacts the positively correlated part f_+ of the biphoton wave function.
- [44] B. Brecht and C. Silberhorn, *Phys. Rev. A* **87**, 053810 (2013).
- [45] X. Sanchez-Lozano, A. B. U'Ren, and J. L. Lucio, *J. Opt.* **14**, 015202 (2012).
- [46] J. Paye, *IEEE J. Quantum Electron.* **28**, 2262 (1992).
- [47] W. H. Zurek, *Nature (London)* **412**, 712 (2001).
- [48] F. Toscano, D. A. R. Dalvit, L. Davidovich, and W. H. Zurek, *Phys. Rev. A* **73**, 023803 (2006).
- [49] L. Olislager, I. Mbodji, E. Woodhead, J. Cussey, L. Furfarò, P. Emplit, S. Massar, K. P. Huy, and J.-M. Merolla, *New J. Phys.* **14**, 043015 (2012).
- [50] Z. Y. Ou and L. Mandel, *Phys. Rev. Lett.* **61**, 54 (1988).
- [51] J. L. O'Brien, A. Furusawa, and J. Vučković, *Nature Photon.* **3**, 687 (2009).